THE JOURNAL OF BIOLOGICAL CHEMISTRY VOL. 286, NO. 39, pp. 34298–34310, September 30, 2011


# Pericellular Versican Regulates the Fibroblast-Myofibroblast Transition

## *A ROLE FOR ADAMTS5 PROTEASE-MEDIATED PROTEOLYSIS*[*S]

Received for publication, April 28, 2011, and in revised form, July 22, 2011 Published, JBC Papers in Press, August 2, 2011, DOI 10.1074/jbc.M111.254938

**Noriko Hattori[‡], David A. Carrino[§], Mark E. Lauer[‡], Amit Vasanji[‡], James D. Wylie[‡], Courtney M. Nelson[‡], and Suneel S. Apte[‡1]**

*From the [‡]Department of Biomedical Engineering, Lerner Research Institute, Cleveland Clinic and the [§]Skeletal Research Center, Department of Biology, Case Western Reserve University, Cleveland, Ohio 44195*

**The cell and its glycosaminoglycan-rich pericellular matrix (PCM) comprise a functional unit. Because modification of PCM influences cell behavior, we investigated molecular mechanisms that regulate PCM volume and composition. In fibroblasts and other cells, aggregates of hyaluronan and versican are found in the PCM. Dermal fibroblasts from *Adamts5*$^{-/-}$ mice, which lack a versican-degrading protease, ADAMTS5, had reduced versican proteolysis, increased PCM, altered cell shape, enhanced α-smooth muscle actin (SMA) expression and increased contractility within three-dimensional collagen gels. The myofibroblast-like phenotype was associated with activation of TGFβ signaling. We tested the hypothesis that fibroblast-myofibroblast transition in *Adamts5*$^{-/-}$ cells resulted from versican accumulation in PCM. First, we noted that versican overexpression in human dermal fibroblasts led to increased SMA expression, enhanced contractility, and increased Smad2 phosphorylation. In contrast, dermal fibroblasts from *Vcan* haploinsufficient (*Vcan*$^{hdf/+}$) mice had reduced contractility relative to wild type fibroblasts. Using a genetic approach to directly test if myofibroblast transition in *Adamts5*$^{-/-}$ cells resulted from increased PCM versican content, we generated *Adamts5*$^{-/-}$;*Vcan*$^{hdf/+}$ mice and isolated their dermal fibroblasts for comparison with dermal fibroblasts from *Adamts5*$^{-/-}$ mice. In *Adamts5*$^{-/-}$ fibroblasts, *Vcan* haploinsufficiency or exogenous ADAMTS5 restored normal fibroblast contractility. These findings demonstrate that altering PCM versican content through proteolytic activity of ADAMTS5 profoundly influenced the dermal fibroblast phenotype and may regulate a phenotypic continuum between the fibroblast and its alter ego, the myofibroblast. We propose that a physiological function of ADAMTS5 in dermal fibroblasts is to maintain optimal versican content and PCM volume by continually trimming versican in hyaluronan-versican aggregates.**

In addition to the role of cells in building specialized structural extracellular matrix, they maintain a pericellular matrix (PCM)[2] that is dynamic, provisional, and intimately associated with the cell surface (1, 2). Thus, it is appropriate to view a cell and its PCM as a functional unit. Processes that could potentially be regulated by PCM include macromolecular assembly (*e.g.* assembly of collagen, fibronectin fibrils, or fibrillin microfibrils), cell surface receptor-ligand interactions, binding of pathogens, and cell-matrix and cell-cell adhesion. PCM is sometimes referred to as the glycocalyx because of its abundant carbohydrate content (3). The PCM in many cell types such as chondrocytes, ova, neurons (in which PCM is also termed the perineuronal net), vascular smooth muscle cells, and fibroblasts contains aggregates of hyaluronan (HA) with chondroitin sulfate proteoglycans (CSPG) (4–7). These aggregates are formed from non-covalent association of HA with large CSPGs such as aggrecan, versican, brevican, and neurocan. In contrast to the aforementioned cell types, heparan sulfate proteoglycans appear to be a critical component of endothelial and osteocyte PCMs (8, 9). The interaction between HA and the CSPG is stabilized by a link protein, and HA is bound to the cell surface via its receptor CD44 (6, 10). In cells robustly synthesizing HA, it can also be tethered to HA synthases (11). HA and cell surface binding of HA are each crucial for the formation of a robust HA-CSPG-rich PCM, as the PCM is eliminated by treatment of cells with hyaluronidase (1, 2).

PCM is invisible by routine light microscopy unless specifically visualized using a particle exclusion assay (1, 2). The ability of the HA-based PCM to exclude particles is based on the cumulative strong negative charge of HA and CS, which leads to a highly hydrated matrix around the cell that excludes particulate matter but not solutes. PCM is consistently well developed in chondrocytes, and the term chondron is used to describe the chondrocyte and its PCM (12). Like chondrocytes, which produce endogenous aggrecan, other cells having CD44 have been shown to assemble large PCMs if provided with exogenous aggrecan and HA (6, 7). Aggrecan is a specialized product of chondrocytes, whereas dermal fibroblasts and vascular smooth muscle cells express a related CSPG named versican (5, 13). In these cells, HA-versican aggregates form a PCM via HA binding to CD44. Through reported interactions with fibrillin-1, tenascin-R, thrombospondin-1, and fibulin-1 and -2, (14–18), versi-

* This work was supported, in whole or in part, by National Institutes of Health Grants AR53890 and HL 107147.

[S] The on-line version of this article (available at http://www.jbc.org) contains supplemental Figs. 1–7.

[1] To whom correspondence should be addressed: Biomedical Engineering-ND20, Cleveland Clinic, 9500 Euclid Ave., Cleveland OH 44195. Tel.: 216-445-3278; Fax: 216-444-9198; E-mail: aptes@ccf.org.

[2] The abbreviations used are: PCM, pericellular matrix; HA, hyaluronan; CSPG, chondroitin sulfate (CS) proteoglycans; GAG, glycosaminoglycan; 4MU, 4-methyumbelliferone; SMA, smooth muscle actin; ADAM, A Disintegrin-like And Metalloprotease with thrombospondin type 1 motif.

can can potentially form a molecular network in the PCM. In contrast to PCM assembly, its turnover has not been extensively studied. However, given the dynamic nature of PCM (2, 13), it is likely that PCM components undergo continuous turnover by cell surface-associated or secreted proteases followed by either release or internalization.

Versican can be expressed as one of four major splice isoforms. The N- and C-terminal globular domains (G1 and G3 respectively) are present in all isoforms, which differ in whether or not alternatively spliced CS-bearing regions (glycosaminoglycan α (GAGα) and GAGβ) are present. Thus, versican V1 contains only the GAGβ domain, V2 contains only the GAGα domain, V0 contains both CS domains, and neither CS-bearing domain is present in V3. Several ADAMTS proteases (*e.g.* ADAMTS1, ADAMTS4, ADAMTS5, ADAMTS9, and ADAMTS20) were previously shown to cleave versican at a specific site, $Glu^{441}$–$Ala^{442}$ within the GAGβ region of versican V1; the corresponding cleaved peptide bond in versican V0 is located between $Glu^{1428}$ and $Ala^{1429}$, as the GAG-β domain lies downstream of the GAGα domain in this isoform (19–22). Proteolysis by these ADAMTS proteases, therefore, has the potential to disrupt the pericellular network formed by versican or to release the CS-bearing regions, resulting in reduced hydration capacity of the PCM. These versican-degrading ADAMTS proteases are all localized in proximity to the cell membrane (22–24) and are, therefore, appropriately placed to regulate PCM versican content. In the present study we determined the consequences of altering the versican content of PCM on dermal fibroblast contractility and investigated the potential role for ADAMTS proteases in versican turnover in the PCM. Because ADAMTS5 has been previously shown to be critical for versican and aggrecan processing and as shown here, is expressed in cultured dermal fibroblasts, we focused on this protease as a tool for modifying versican turnover. Studies described herein using cultured dermal fibroblasts from *Adamts5*$^{-/-}$ and *Vcan*-deficient mice suggest a critical role for pericellular versican in regulating cell behavior and also demonstrate that ADAMTS5 has a critical role in versican turnover in fibroblasts. In the presence of excess pericellular versican or when versican turnover is reduced after *Adamts5* inactivation, dermal fibroblasts undergo transition to a myofibroblast-like cell, a cellular phenotype that is of high significance for wound healing and fibrosis.

## EXPERIMENTAL PROCEDURES

Unless otherwise specified, reagents were obtained from Sigma.

*Transgenic Animals, Dermal Fibroblast Isolation, and Transfection*—Mice with targeted inactivation of *Adamts5* (B6.129P2-*Adamts5*$^{tm1Dgen}$/J, referred to here as *Adamts5*$^{-/-}$), were obtained from The Jackson Laboratory (Bar Harbor, ME). The *Adamts5*-targeted allele was subsequently backcrossed for 10 consecutive generations into the C57Bl/6 strain so as to be essentially congenic in this strain (25). The mouse *Vcan*$^{hdf}$ allele (26) is an insertional mutant that abrogates expression of all versican isoforms and was also maintained in the C57Bl/6 strain. *Vcan*$^{hdf/hdf}$ mouse embryos die around 9.5 days of gestation; hence, only *Vcan*$^{hdf/+}$ mice were used for these studies. Mice were housed in the Biological Resources Unit of the Cleveland Clinic according to a protocol approved by the Institutional Animal Care and Use Committee under controlled light/dark and temperature conditions and provided with food and water *ad libitum*. PCR of DNA obtained from tail biopsies was used for genotyping. *Adamts5*$^{-/-}$ mice were obtained by breeding hemizygous mice. *Adamts5*$^{-/-}$;*Vcan*$^{hdf/+}$ mice were obtained by crossing *Adamts5*$^{-/-}$ and *Adamts5*$^{+/-}$;*Vcan*$^{hdf/+}$ mice. Animal tissues were obtained at post-mortem after euthanasia, performed as per the recommendations of the American Veterinary Association Panel on Euthanasia.

*Cell Culture*—Dermal fibroblasts were isolated from skin by outgrowth from skin explants obtained post-mortem from 3-week-old mice. These were further cultured for at least 5 passages before experimental use. In some experiments cells were cultured for 24 h in the presence of either 500 μM 4-methyumbelliferone (4MU) to suppress HA synthesis or the TGFβ type I receptor (ALK5) inhibitor SB431542 (Sigma, catalogue no. S4317), used at 10 μM to block TGFβ receptor signaling. In these experiments cell viability was determined using the trypan blue assay, and no toxicity of these compounds was seen. For versican overexpression, human neonatal dermal fibroblasts (catalogue no. C0045C: Invitrogen) were transfected with 5 μg of a versican V1 expression plasmid (in pSecTag2 Invitrogen) or with the empty pSecTag2 vector using the Amaxa nucleofector and a human dermal fibroblast nucleofector kit according to the manufacturer's protocols (Lonza Walkersville, Inc, Walkersville, MD). The cells were passaged into 10-cm plates 24 h after transfection and were used in a collagen gel contraction assay (described below) after an additional 48 h in culture. Successful versican transfection was confirmed by Western blotting of cell lysates using rabbit anti-mouse versican polyclonal antibody (1:1000 dilution; catalogue no. AB1033, Millipore Inc, Billerica, MA).

To provide a source of exogenous ADAMTS5, we collected the medium from human chondrosarcoma-derived HTB-94 cells (ATCC, Manassas, VA) stably transfected with plasmid constructs expressing active ADAMTS5 (wild type (WT) medium) or catalytically inactive mutant ADAMTS5 having an E441A substitution in the active site (EA medium) and medium from empty vector-transfected cells as the control. *Adamts5*$^{-/-}$ and WT dermal fibroblasts were cultured with these media (blended 1:1 with fresh medium) for 24 h before analysis.

*Reverse Transcription-PCR (RT-PCR)*—Total RNA was extracted from skin and cultured dermal fibroblasts of 3-week-old WT mice using TRIzol. The RNA was reverse-transcribed using the SuperScript II cDNA synthesis kit (Stratagene, Santa Clara, CA). PCR was done using TaqDNA polymerase (Apex, Genesee Scientific, San Diego, CA) with the following conditions: 95 °C for 2 min, 95 °C for 30 s, 60 °C for 30 s, 72 °C for 30 s for 40 cycles followed by a final extension step of 72 °C for 10 min. ADAMTS oligonucleotide primer sequences were previously published (25).

For RT-PCR analysis of the genes encoding HA synthases *Has1*, *Has2* and *Has3*, the primer sequences were as previously described (27). PCR was done using the following conditions: 95 °C for 2 min, 95 °C for 30 s, 55 °C for 30 s, 72 °C for 30 s for 40

cycles followed by a final extension step of 72 °C for 10 min. PCR products were analyzed by electrophoresis in 2% agarose gels.

*β-Galactosidase Staining*—Cultured fibroblasts were fixed using freshly prepared 4% paraformaldehyde prepared in β-galactosidase wash buffer (0.1 M phosphate buffer, pH 7.4, 2 mM $MgCl_2$, 0.01% sodium deoxycholate, 0.02% (v/v) Nonidet P-40), rinsed in the wash buffer, and incubated for 2 h at 37 °C in β-galactosidase staining solution as previously described (28). After a brief rinse in wash buffer, the fibroblasts were photographed on an inverted microscope.

*In Vitro Fibroblast Proliferation and Migration Assays*—Proliferation of dermal fibroblasts from *Adamts5*$^{-/-}$ and WT littermates was measured using 5-bromo-2′-deoxyuridine (BrdU) Labeling and Detection Kit III (Roche Applied Science). Cells were serum-starved for 24 h to achieve growth arrest, and the medium was subsequently changed to DMEM containing 1% fetal bovine serum. After 6 h, 10 mM BrdU was added to the medium, and cells were cultured for an additional 42 h before undertaking the assay as per the manufacturer's instructions.

For analysis of cell migration, dermal fibroblasts were cultured from dermal explants of 3-week-old *Adamts5*$^{-/-}$ and WT littermates in DMEM containing 10% FBS. Fibroblasts were grown to confluence on 12-well plates (BD Biosciences). Before the migration assay, they were cultured in serum-free medium overnight and treated for 2 h with 10 ng/ml mitomycin C, an inhibitor of cell proliferation. The confluent monolayer was scratched with a 200-μl polypropylene pipette tip. The resulting "scratch wound" was photographed every 5 min by time-lapse photomicroscopy as previously described (29).

*Proteoglycan Isolation and Analysis*—Skin of comparable wet weight was isolated from two pairs of *Adamts5*$^{-/-}$ and WT littermates shortly after death, minced, and extracted with guanidinium chloride as previously described (30). Proteoglycans were isolated by step elution anion exchange chromatography on diethylaminoethyl (DEAE)-Sephacel as previously described (30). The step elutions consisted of 0.25 M NaCl (DEAE pool 1) and 1.0 M NaCl (DEAE pool 2). DEAE pool 1 contains HA, some glycoproteins, and also the DPEAAE fragment of versican V1 that lacks CS chains and, therefore, does not bind to DEAE-Sephacel; DEAE pool 2 contains sulfated proteoglycans including versican and the DPEAAE fragment of versican V0 (30, 31). The amounts of glycosaminoglycans in each of the DEAE pools were determined by the Safranin O assay (32). Proteoglycans were analyzed on Western blots as done previously (30, 31). For SDS-PAGE, equal amounts of total glycosaminoglycans per sample (as determined from the Safranin O assay) were loaded for comparison of *Adamts5*$^{-/-}$ and WT littermates. DEAE pool 2 was electrophoresed after treatment with chondroitinase ABC to generate core proteins (30, 33). DEAE pool 1 was electrophoresed without prior chondroitinase treatment, as the DPEAAE fragment of V1 lacks CS (31).

*Fluorophore-assisted Carbohydrate Electrophoresis*—The fluorophore-assisted carbohydrate electrophoresis method for the quantification of HA is described elsewhere (34). Briefly, the medium was removed, and the cells were washed with PBS followed by digestion with proteinase K. HA was purified by ethanol precipitation, digested to disaccharides with hyaluronidase standard deviation, and labeled with 2-aminoacridone. The samples were electrophoresed on a polyacrylamide gel, and the HA disaccharide band was imaged on an ultraviolet transilluminator and quantified using gel imaging software.

*Cell Shape Analysis*—Fibroblasts were cultured with 1 μM calcein (catalogue no. C3099, calcein AM; Invitrogen) for 30 min, and the cells were washed and photographed using an inverted, wide-field Leica fluorescence microscope (DM IRB, Heidelberg, Germany), a Q-Imaging CCD camera (Retiga-SRV, Surrey, BC), and a 10× or 20× objective. Morphometric analysis of cell shape parameters was done in batch for all images within a particular group (WT *versus* littermate) using custom semi-automated scripts generated in Image-Pro Plus v6.2 (Media Cybernetics, Silver Spring, MD). Briefly, for each cell within a given image, a region of interest was created along its boundary using a wand tool (single-click operation by a "blinded" observer). Each region of interest was then used to create a binary cell mask that was subsequently analyzed to extract and automatically export various morphological parameters including area, aspect ratio, roundness, perimeter, convex perimeter, and min/max/mean Feret diameter.

*Western Blot Analysis*—Fibroblasts were obtained from WT, *Adamts5*$^{-/-}$ and *Vcan*$^{hdf/+}$ mice. Cell monolayers (including extracellular matrix) were scraped off tissue culture surfaces and lysed in T-PER Tissue Protein Extraction Reagent (Thermo Scientific, Rockford, IL) with protease inhibitor mixture (Roche Applied Science). Alternatively, cells were lysed by incubation in 2× Laemmli sample buffer. Lysis in radioimmunoprecipitation buffer (Santa Cruz) was used for sample preparation for Western blotting of phosphorylated proteins. Proteins were separated by reducing SDS-PAGE and transferred to a polyvinylidene fluoride membrane for Western blotting using either enhanced chemiluminescence or a colorimetric method that utilized alkaline phosphatase-conjugated secondary antibody. The following antibodies were used: rabbit polyclonal anti-DPEAAE, which recognizes the new C terminus of the N-terminal versican fragment resulting from cleavage at the $Glu^{441}$-$Ala^{442}$ peptide bond, but not uncleaved versican (1:2000 dilution; Affinity BioReagents, Golden, CO), rabbit polyclonal anti-versican GAGβ domain antibody, recognizing intact versican V0 or V1 isoforms (1:1000 dilution; catalogue no. AB1033, Millipore), mouse monoclonal anti-α smooth muscle actin (SMA) antibody (1:1000 dilution; catalogue no. A2547), rabbit polyclonal anti-Smad2/3 antibody (1:1000; catalogue no. 3102 Cell Signaling), rabbit polyclonal anti-pSmad2/3 antibody (1:200; catalogue no. sc-11769, Santa Cruz), rabbit polyclonal anti-fibronectin (Abcam, Cambridge, MA; catalogue no. ab23750), rabbit polyclonal anti-Smad2 antibody (1:1000; catalogue no. 3103 Cell Signaling), rabbit polyclonal anti-pSmad2 antibody (1:1000; catalogue no. 3101 Cell Signaling), rabbit polyclonal anti-ERK antibody (1:200; catalogue no. sc-94; Santa Cruz), rabbit polyclonal anti-pERK antibody (1:200; catalogue no. sc-7383; Santa Cruz), or mouse monoclonal anti-GAPDH antibody (1:300 dilution; catalogue no. MAB374; Millipore). For quantification of Western blot signal intensities, the blots were scanned, and the signal intensities were normalized to GAPDH signal intensities on the same blots.

*Particle Exclusion Assay*—The exclusion of red blood cells (RBCs) was used to visualize PCM. Formalin-fixed sheep RBCs (Inter-Cell Technologies Inc. Jupiter, FL) were washed in PBS followed by centrifugation at 1000 × *g* for 10 min at least four times. The pellet was resuspended in medium to obtain a concentration of $1.0 \times 10^8$ RBCs/ml. Dermal fibroblasts were plated at a sparse (non-confluent) density in 6-well plates in serum-free medium for 24 h, and 200 μl of the RBC suspension was added to each well. The plates were incubated at 37 °C for 15 min to allow the RBCs to settle around the cells. For hyaluronidase digestion, fibroblasts were cultured in the presence or absence of 0.5 units/ml *Streptomyces* hyaluronidase for 1 h before conducting the particle exclusion assay.

For quantification of the area of PCM, images of calcein-labeled cells surrounded by RBCs were acquired using an inverted, wide-field Leica microscope (DM IRB, Heidelberg, Germany), Q-Imaging CCD camera (Retiga-SRV, Surrey, BC), and a 20× objective in both phase-contrast and fluorescence modes. Analysis of "exclusion" regions (void areas surrounding cells in which particles were absent) was performed in batch mode using custom, fully automated scripts generated in Image Pro Plus v6.2 (Media Cybernetics, Silver Spring, MD). Briefly, phase-contrast and corresponding fluorescence images of cells were loaded together into Image Pro. Particles were segmented from the phase-contrast images by applying a "top-hat" morphological filter (which preferentially enhances the central portion of each particle) that enabled application of a fixed intensity threshold. Similarly, binary cell masks were created using a single-value intensity threshold after application of a large spectral high-pass filter. Cell masks were then subtracted from the binarized particle masks to remove any contribution of cell surface-bound particles. Using a "thinning" operation, cell masks were reduced to one-pixel-width medial lines. For every pixel along the cell medial axis, the angle and distance to every particle centroid was calculated (polar coordinate system conversion). Then, for a 360-degree rotation around each medial axis pixel (5-degree steps, 20-degree range), the closest particle location was recorded. After a full rotation around each medial axis point, recorded points were connected to produce the exclusion area around that particular pixel. A final image of the cell exclusion area was generated by repeating this process for the entire medial axis, filling holes, and subtracting the cell area mask. To determine mean exclusion length (exclusion mask thickness), a skeleton of the exclusion mask was multiplied by its Euclidean distance map. Mean exclusion length was then calculated by summing the resultant pixel intensities, dividing by the total skeletal length, and multiplying by a factor of two. This parameter along with cell/exclusion area and perimeter were automatically exported to Excel for each image analyzed. The PCM area was quantified for randomly chosen cell images.

*In Vitro Collagen Gel Contraction Assay*—The collagen gel contraction assay was used as a measure of cell contractility. Collagen gel contraction assays were performed in 24-well tissue culture plates. Circular agarose molds were prepared using 10-mm diameter cloning cylinders (ThermoFisher Scientific, Pittsburgh, PA) and 3% agarose solution. A solution of rat-tail collagen (catalogue no. 354236; BD Bioscience) was mixed with dermal fibroblasts ($3 \times 10^5$/ml) suspended in DMEM supplemented with 10% FBS and antibiotics, and the fibroblast-collagen mixture was pipetted into circular agarose molds of 24-well tissue culture plates (Corning, Ithaca, NY). Gels were polymerized at 37 °C for 1 h, overlaid with 1 ml of DMEM, 10% FBS with antibiotics, gently detached from the sides and bottom of the mold with a spatula, and allowed to contract as suspended gels for 16 h. In some experiments cells were cultured for 24 h with addition of 4MU or SB431542 to the culture medium at concentrations stated above. These inhibitors were also present during the collagen gel contraction assay. The gels were photographed under a stereomicroscope upon conclusion of the assay; the gel area was measured using Image J software (NIH, Bethesda, MD) and expressed as a percentage of the area of the well.

*Immunofluorescence and Actin Labeling*—Cells were grown to 70% confluence in 12-well plates (Corning, Ithaca, NY) and cultured in serum-free medium for 24 h. The cells were washed with PBS and fixed in 100% ethanol for 5 min at room temperature. After fixation the wells were washed three times with PBS and incubated with anti-SMA (1:100 dilution) overnight and subsequently with anti-mouse Alexa 488 (1:500; Molecular Probes, Eugene, OR) and fluorescein isothiocyanate (FITC)-labeled phalloidin. After washing, the cells were coverslipped with Vectashield Fluorescent Mounting Medium with DAPI (Vector Laboratories, H-1200) and photographed.

*Statistical Analysis*—Statistical differences were determined using Student's *t* test (unpaired). *p* values less than 0.05 were considered significant.

## RESULTS

*Adamts5 Is Strongly Expressed in Dermal Fibroblasts in Vitro and in Vivo*—To evaluate the expression of ADAMTS proteases that could potentially alter versican levels in fibroblast PCM, we isolated RNA from cultured dermal fibroblasts and mouse skin, both obtained from WT mice at 3 weeks of age, and used RT-PCR for detection of relevant ADAMTS transcripts. In skin, *Adamts5* mRNA was most strongly expressed, although *Adamts1* and *Adamts4* mRNA were also detected (Fig. 1*A*, *upper panel*). In dermal fibroblasts from these mice, *Adamts5* was also more strongly expressed than the others; *Adamts1*, *Adamts4*, and *Adamts8* mRNA were also detected (Fig. 1*A*, *lower panel*). We also used β-galactosidase staining of cultured dermal fibroblasts enabled by the intragenic *lacZ* cassette inserted during construction of the *Adamts5* targeting vector in which β-galactosidase is targeted to the nucleus by a nuclear localization signal. Fibroblasts from $Adamts5^{-/-}$ dermis had nuclear β-galactosidase staining, indicative of continued expression of *Adamts5* in monolayer culture, whereas WT fibroblasts did not (Fig. 1*B*). In addition to suggesting a potential physiological role for ADAMTS5 in the dermis of skin, these data showed that a potential role of *Adamts5* in remodeling pericellular versican could be investigated in cultured dermal fibroblasts.

*Versican Cleavage Is Reduced in $Adamts5^{-/-}$ Fibroblasts and Is Associated with Enhanced PCM*—To determine whether there was altered versican turnover in $Adamts5^{-/-}$ skin, we analyzed total skin proteoglycans isolated from these mice and from WT littermates ($n = 2$ mice each). Analysis of pool 1 and

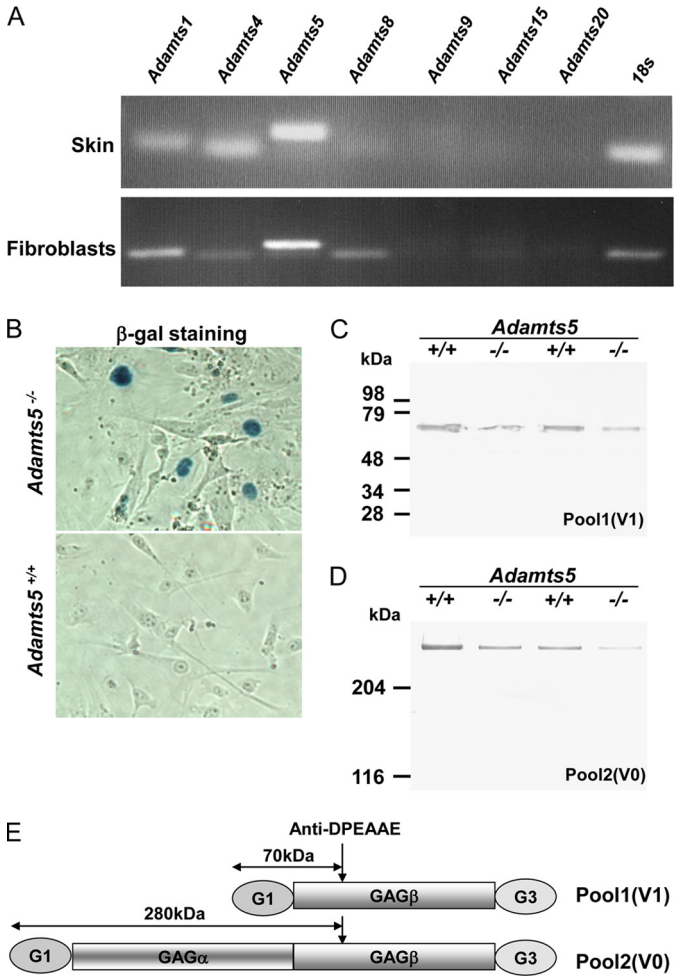


FIGURE 1. **Mouse dermal fibroblasts express *Adamts5* and two versican isoforms.** *A*, RT-PCR analyses of 3-week-old mouse skin RNA (*upper panel*) and of cultured WT dermal fibroblast RNA (*lower panel*) show expression of *Adamts5* in RNA samples from both sources. *Adamts1*, *Adamts4*, and *Adamts8* mRNA were also detectable in cultured fibroblasts. 18 S RNA PCR was used as a control for PCR amplification. *B*, β-galactosidase histochemistry of cultured WT and *Adamts5*$^{-/-}$ dermal fibroblasts shows nuclear β-galactosidase staining of *Adamts5*$^{-/-}$ dermal cells (*blue nuclei*) but not WT dermal cells. *C* and *D*, anti-DPEAAE Western blot of proteoglycans isolated from the skin of mice of the indicated phenotypes in pairwise analysis of *Adamts5*$^{-/-}$ mice and WT littermates is shown. The distinction between pool 1 and pool 2 is explained under "Experimental Procedures." The DPEAAE-reactive cleaved versican arising from the V1 isoform (*pool 1*) and the V0 isoform (*pool 2*) is reduced in *Adamts5*$^{-/-}$ mice when compared with WT littermates. *E*, graphic representation of the molecular species identified in pool 1 and pool 2 is shown.

pool 2, which contain ADAMTS-processed versican V1 and V0, respectively, showed that *Adamts5*$^{-/-}$ skin had less of the respective anti-DPEAAE-reactive cleavage product (70 kDa for versican V1, >250 kDa for versican V0) as a proportion of total proteoglycan than the corresponding WT littermate (Fig. 1, *C–E*).

Skin is a composite of different cell types, including keratinocytes, endothelial cells, fibroblasts, and smooth muscle cells. To determine whether the observed changes in versican processing were present in dermal fibroblasts, we isolated dermal fibroblasts for specific analysis of versican turnover from three pairs of *Adamts5*$^{-/-}$ mice and WT littermates. Western blot analysis using the anti-DPEAAE antibody demonstrated that *Adamts5*$^{-/-}$ fibroblast monolayers had greatly reduced content of the expected 70-kDa ADAMTS-cleaved versican product, which was statistically significant (Fig. 2*A*, *right-hand panel*). A representative Western blot is shown in Fig. 2*A*, *left-hand panel*. This suggested that ADAMTS5 had a critical role in versican turnover in dermal fibroblasts. Conversely, the anti-GAGβ antibody demonstrated higher levels of intact versican in extracts of monolayers of *Adamts5*$^{-/-}$ cells, which was also statistically significant (Fig. 2*B*, *right-hand panel*). A representative Western blot is shown in Fig. 2*B*, *left-hand panel*. Consistent with these observations of reduced versican processing and increased intact versican, particle exclusion assays showed enhanced PCM around *Adamts5*$^{-/-}$ fibroblasts (Fig. 2*C*, *arrows*). Quantification of the PCM around *Adamts5*$^{-/-}$ and WT cells showed an enhancement of the zone of RBC exclusion around *Adamts5*$^{-/-}$ dermal fibroblasts that was statistically significant (Fig. 2*D*, *left-hand panel*). The quantified difference was also statistically significant when the area of the exclusion zone was normalized to the cell perimeter, to take into account the observed cell shape differences between WT and *Adamts5*$^{-/-}$ dermal fibroblasts (Fig. 2*D*, *right-hand panel* and supplemental Fig. 1).

*Adamts5*$^{-/-}$ *Fibroblasts Have Altered Cell Shape but Retain Normal Migration and Proliferation*—Because phase contrast microscopy suggested an altered cell shape of *Adamts5*$^{-/-}$ fibroblasts, we live-stained cells with calcein, a fluorescent dye that outlines cellular boundaries. Imaging and subsequent analysis of these cells indicated that on average, *Adamts5*$^{-/-}$ fibroblasts had a different shape from WT fibroblasts (supplemental Fig. 1, *A* and *B*). Morphometric analysis indicated that *Adamts5*$^{-/-}$ fibroblasts had an expanded surface area and a significantly reduced minor/major aspect ratio, which is a measure of the degree of spreading (supplemental Fig. 1*B*). Because of a potential role for both the PCM and proteases in cell migration, we quantified the migration of fibroblasts across a scratch wound created in dermal fibroblast monolayer cultures, but no significant difference was seen between *Adamts5*$^{-/-}$ and WT fibroblasts (data not shown). No significant difference was seen in proliferation rates of *Adamts5*$^{-/-}$ and WT fibroblasts (supplemental Fig. 1*C*) or in levels or proteolysis of fibronectin, a key adhesive protein (data not shown).

By adding exogenous active ADAMTS5 to *Adamts5*$^{-/-}$ fibroblasts, the altered cell shape in these cells was reversed to resemble that of WT fibroblasts, whereas catalytically inactive ADAMTS5 did not have this effect (supplemental Fig. 2, *A* and *B*).

*Adamts5*$^{-/-}$ *Dermal Fibroblasts Are Myofibroblastic*—Because of the altered shape of *Adamts5*$^{-/-}$ fibroblasts, we first evaluated the actin cytoskeleton using phalloidin-FITC staining without noting consistent differences (not shown). However, Western blot analysis of SMA showed significantly higher expression by *Adamts5*$^{-/-}$ fibroblasts compared with WT (Fig. 3, *A* and *B*). This was confirmed by immunofluorescence microscopy (supplemental Fig. 3). Because SMA expression is related to cell contractility, we compared *Adamts5*$^{-/-}$ fibroblasts with WT fibroblasts in contraction of a collagen gel. *Adamts5*$^{-/-}$ fibroblasts consistently contracted collagen gels to a greater extent than WT cells, and the reduction in collagen gel surface area was statistically significant (Fig. 3, *C* and *D*).

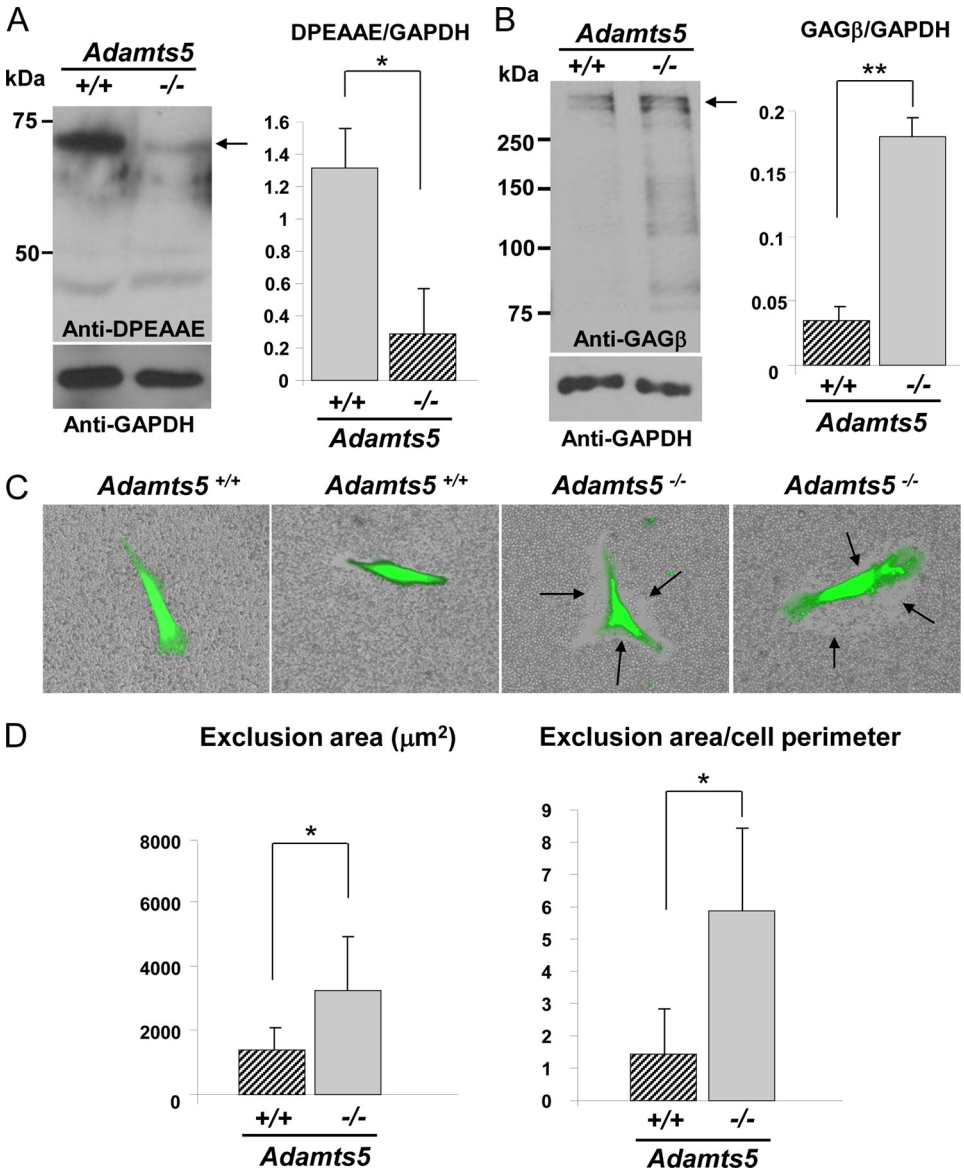


FIGURE 2. **Reduced versican processing and accumulation of the PCM around cultured *Adamts5*$^{-/-}$ dermal fibroblasts.** *A*, *left-hand panel*, a Western blot using anti-DPEAAE identified a 70-kDa reactive species (*arrow*) in WT fibroblast extracts, but this was greatly reduced in null fibroblasts. The 40-kDa species is nonspecific. The *lower immunoblot* shows a Western blot with GAPDH as a control (representative of $n = 3$). *Right-hand panel*, quantification of anti-DPEAAE Western blots after normalization to GAPDH shows a statistically significant difference between *Adamts5*$^{-/-}$ and WT fibroblasts (*, $p < 0.01$). *B*, *left-hand panel*, Western blot with an antibody to versican (anti-GAG$\beta$) identified a higher amount of intact versican (*arrow*) in null fibroblasts compared with wild type. The *lower panel* shows a Western blot with GAPDH as a control. Versican migrates as a ~350-kDa species when deglycosylated with chondroitinase ABC (representative of $n = 4$). The observed ~350 kDa doublet may be a mixture of intact versican V1 and versican V1 lacking the N-terminal 70-kDa species. *Right-hand panel*, quantification of anti-GAG$\beta$ Western blots after normalization to GAPDH shows a statistically significant difference between *Adamts5*$^{-/-}$ and WT fibroblasts (**, $p < 0.05$). *C*, exclusion of RBCs around calcein-labeled fibroblasts shows accumulation of PCM around fibroblasts (representative of $n = 25$). The exclusion zone is indicated by *arrows*. *D*, quantification of the area of RBC exclusion (*left-hand panel*) and of the ratio of the exclusion area to cell perimeter (*right-hand panel*) shows increased PCM around *Adamts5*$^{-/-}$ dermal fibroblasts ($n = 25$). *Error bars* indicate S.D.

Taken together, the higher expression level of SMA and greater contractility strongly suggested that *Adamts5*$^{-/-}$ fibroblasts had assumed a myofibroblast phenotype. Because previous work noted a strong association between the activation of TGF$\beta$ signaling and the myofibroblast phenotype, we evaluated this signaling pathway. Western blotting showed higher pSmad2/3 levels in *Adamts5*$^{-/-}$ fibroblasts than in WT fibroblasts, whereas the level of pERK was unchanged (Fig. 3, *E* and *F*). Additional evidence that this myofibroblastic phenotype was dependent on TGF$\beta$ signaling was provided by the effect of a TGF$\beta$ receptor-blocking agent. In the presence of this agent, there was reduced expression of SMA (Fig. 3, *G* and *H*) as well as reduced collagen gel contractility (Fig. 3, *I* and *J*).

Furthermore, the addition of active ADAMTS5-containing medium to *Adamts5*$^{-/-}$ fibroblasts led to a reduction of Smad2 phosphorylation in these cells, whereas this effect was not seen upon the addition of inactive ADAMTS5-containing medium (supplemental Fig. 2*C*). Although isolated *Adamts5*$^{-/-}$ fibroblasts consistently had up-regulated SMA levels, no alteration of SMA staining (number, distribution, or type of labeled cells) was seen in intact skin of *Adamts5*$^{-/-}$ and WT mice (supplemental Fig. 4).

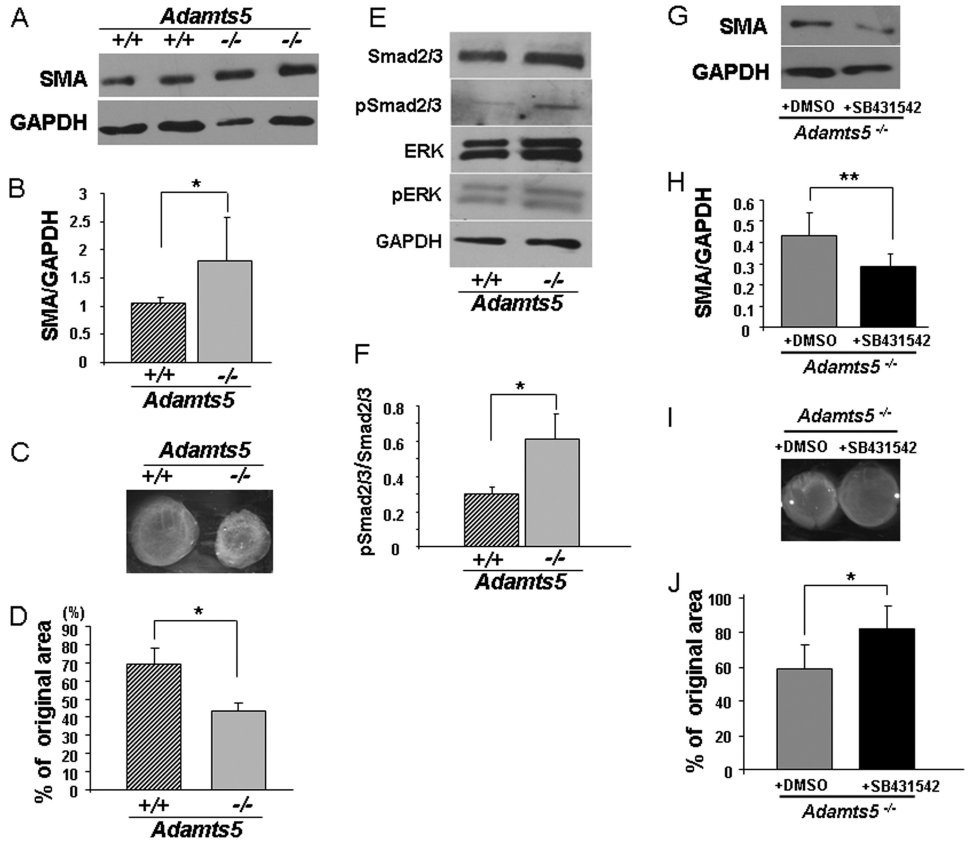


FIGURE 3. ***Adamts5*$^{-/-}$ dermal fibroblasts show features of myofibroblasts.** *A*, Western blot for SMA shows increased levels in *Adamts5*$^{-/-}$ dermal fibroblasts (−/−) compared with WT (+/+) (representative of three biological replicates and five technical replicates). *B*, results of densitometric analysis of SMA Western blots show a statistically significant increase in *Adamts5*$^{-/-}$ dermal fibroblasts (*, $p < 0.01$). *C*, a collagen gel contraction assay (representative example) shows the greater contractility of *Adamts5*$^{-/-}$ dermal fibroblasts. *D*, quantification of gel contraction assay shows a statistically significant difference (*, $p < 0.01$) in contractility between *Adamts5*$^{-/-}$ and WT dermal fibroblasts ($n = 3$ biological replicates, 4 technical replicates, and triplicate wells per experiment). *E*, Western blot analyses with the indicated antibodies show increased pSmad levels but no change in pERK in *Adamts5*$^{-/-}$ dermal fibroblasts (representative of $n = 3$). *F*, quantification by densitometric analysis of pSmad2/3 to total Smad2/3 shows a statistically significant difference between *Adamts5*$^{-/-}$ and WT dermal fibroblasts (*, $p < 0.01$) ($n = 3$ biological replicates). *Error bars* indicate S.D. *G*, *Adamts5*$^{-/-}$ cells were treated with SB431542, which led to decreased expression of SMA (representative of $n = 3$). *H*, quantification of SMA showed statistically significant reduction by 4MU-treated cells (**, $p < 0.05$). *I*, the collagen gel contraction assay was done using *Adamts5*$^{-/-}$ cells treated with SB431542 or with DMSO (vehicle for SB431542 delivery) as a control. *J*, a statistically significant reduction of contractility was observed in SB431542-treated *Adamts5*$^{-/-}$ cells (*, $p < 0.01$, $n = 3$). *Error bars* indicate S.D.

*The Enhanced PCM of Adamts5*$^{-/-}$ *Dermal Fibroblasts Is HA-based*—Increased pericellular HA was previously implicated in the myofibroblast transition (35). Thus, the association of increased PCM in *Adamts5*$^{-/-}$ fibroblasts with myofibroblast transition led us to ask whether this PCM was also HA-based. Fluorophore-assisted carbohydrate electrophoresis analysis of HA content of cell monolayers did not show a significant difference between *Adamts5*$^{-/-}$ and WT fibroblasts nor was there any change of *Has1* and *Has2* expression between these cells (supplemental Fig. 5, *A* and *B*). However, we found that treatment of *Adamts5*$^{-/-}$ fibroblasts with *Streptomyces* hyaluronidase (which degrades HA but not chondroitin sulfate) led to loss of the PCM (Fig. 4*A*). Inclusion of 0.2 units/ml hyaluronidase in the cultures undergoing collagen gel contraction led to statistically significant reduction of the enhanced contractility seen in *Adamts5*$^{-/-}$ fibroblasts (Fig. 4, *B* and *C*). In addition, treatment of *Adamts5*$^{-/-}$ dermal fibroblasts with 500 $\mu$M 4MU, which interferes with HA synthesis, led to reduction of SMA expression (Fig. 4, *D* and E) as well as reduced contractility (Fig. 4, *F* and *G*). We confirmed that cell viability was unaffected by 4MU treatment compared with untreated cultures using the trypan blue exclusion assay (data not shown). These observations showed that reduction of HA, which is predicted to lead to reduction of pericellular versican binding capacity, could ameliorate the phenotype of *Adamts5*$^{-/-}$ dermal fibroblasts. Furthermore, these findings are consistent with previous work showing that enhanced HA synthesis and incorporation into PCM was associated with a myofibroblast phenotype (35), as an increase in HA would not only increase the volume of PCM but could conceivably also increase versican binding capacity and/or the amount of bound versican.

*Modulation of Fibroblast Versican Gene Dosage Affects the Fibroblast-Myofibroblast Transition*—To address potential mechanisms by which ADAMTS5-mediated versican proteolysis influenced cell behavior, we considered two possibilities.

We first addressed the possibility that ADAMTS5-mediated clearance of versican in PCM constituted a key mechanism. We asked whether versican haploinsufficient dermal fibroblasts differed in their phenotype from their WT-littermate counterparts. Indeed, *Vcan*$^{hdf/+}$ dermal fibroblasts had significantly reduced SMA expression (Fig. 5, *A* and *B*) and, corresponding to this, significantly reduced contractility of collagen gels (Fig.

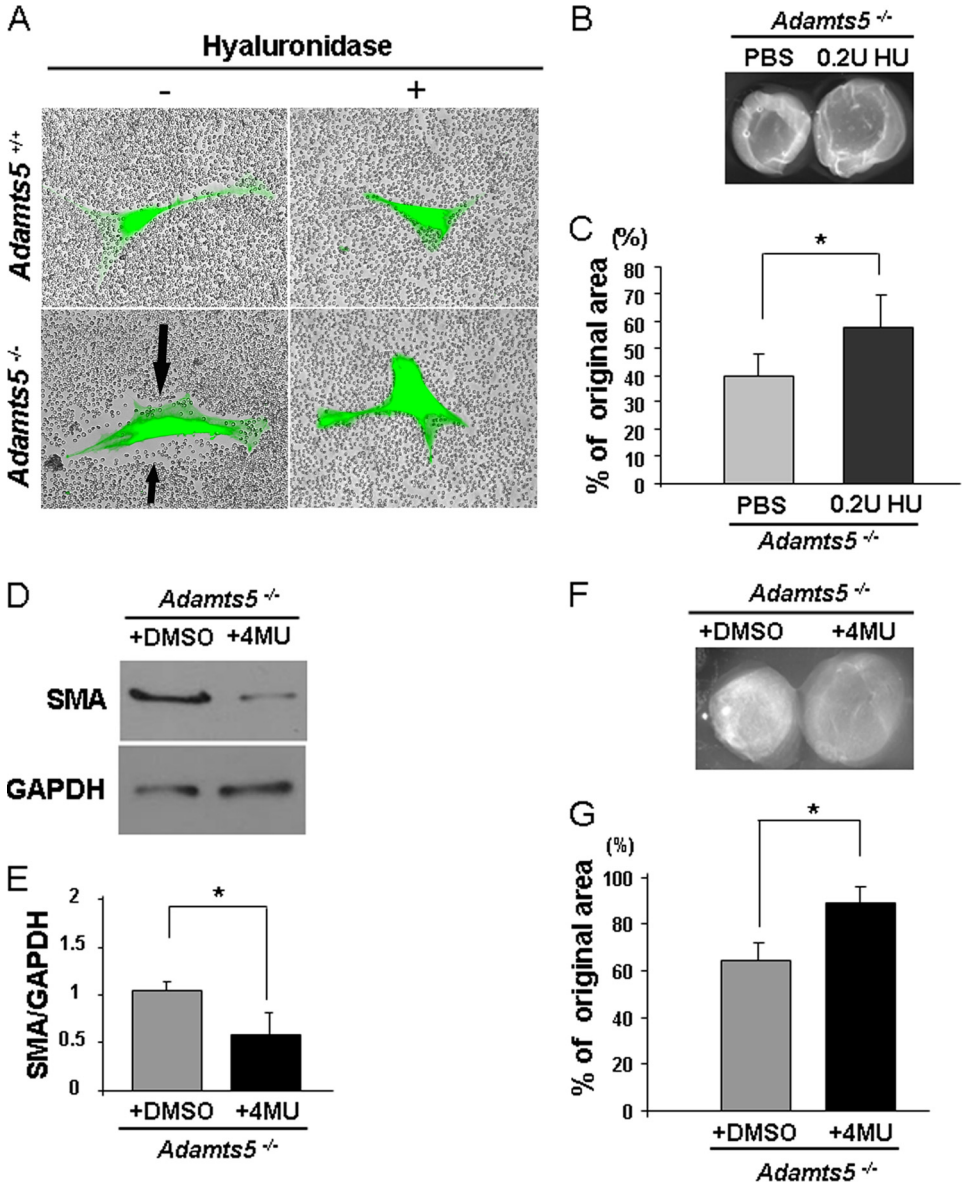


FIGURE 4. **The increased PCM and altered phenotype of *Adamts5*$^{-/-}$ dermal fibroblasts can be modulated by HA content.** *A*, treatment of *Adamts5*$^{-/-}$ or WT dermal fibroblasts with *Streptomyces* hyaluronidase (+) leads to loss of the PCM seen in untreated *Adamts5*$^{-/-}$ cells (−, *arrows*) as shown by the RBC assay (representative of $n = 3$). *B*, *Adamts5*$^{-/-}$ dermal fibroblasts embedded in collagen gels and cultured in the presence of 0.2 units (*U*)/ml hyaluronidase showed reduced contractility compared with untreated *Adamts5*$^{-/-}$ dermal fibroblasts. *C*, quantification of collagen gel contraction shows statistically significant reduction in contractility in *Adamts5*$^{-/-}$ cells treated with hyaluronidase (*, $p < 0.01$) (2 independent experiments with four replicates each). *D*, *Adamts5*$^{-/-}$ cells were treated with 4MU, which led to decreased expression of SMA (representative of $n = 3$). *E*, quantification of SMA showed statistically significant reduction in contractility by 4MU-treated cells (*, $p < 0.01$). *F*, the collagen gel contraction assay was done using *Adamts5*$^{-/-}$ cells treated with 4MU or with DMSO (vehicle for 4MU delivery) as a control. *G*, a statistically significant reduction of contractility was observed in 4MU-treated *Adamts5*$^{-/-}$ cells (*, $p < 0.01$, $n = 3$). *Error bars* indicate S.D.

5, *C* and *D*). Furthermore, *Vcan*$^{hdf/+}$ dermal fibroblasts also had reduced TGFβ signaling as shown by decreased cellular levels of phosphorylated Smad protein (Fig. 5, *E* and *F*).

Next, we isolated fibroblasts from *Adamts5*$^{-/-}$;*Vcan*$^{hdf/+}$ mice and asked whether introduction of *Vcan* haploinsufficiency in an *Adamts5*$^{-/-}$ genetic background could ameliorate enhanced SMA expression and enhanced contractility of *Adamts5*$^{-/-}$ fibroblasts. *Adamts5*$^{-/-}$;*Vcan*$^{hdf/+}$ cells showed reduced versican production compared with *Adamts5*$^{-/-}$ cells (supplemental Fig. 6*A*). This reduction of versican gene dosage also decreased the increased SMA expression (Fig. 6, *A* and *B*) and decreased the contractility of *Adamts5*$^{-/-}$ cells (Fig. 6, *C* and *D*) and the amount of cellular pSmad2 (Fig. 6, *E* and *F*). Second, we asked whether the lack of a product of versican proteolysis could lead to myofibroblast transition. Because previous work suggested a bioactive role for the G1-DPEAAE$^{441}$ N-terminal fragment derived from versican V1 processing in interdigital web regression (25), we tested whether adding the fragment to *Adamts5*$^{-/-}$ cells could ameliorate the myofibroblast phenotype. However, inclusion of this fragment during the gel contraction assay was without a significant effect (supplemental Fig. 6*B*).

To complement these loss-of-function approaches, we raised cellular versican levels in human dermal fibroblasts via tran-

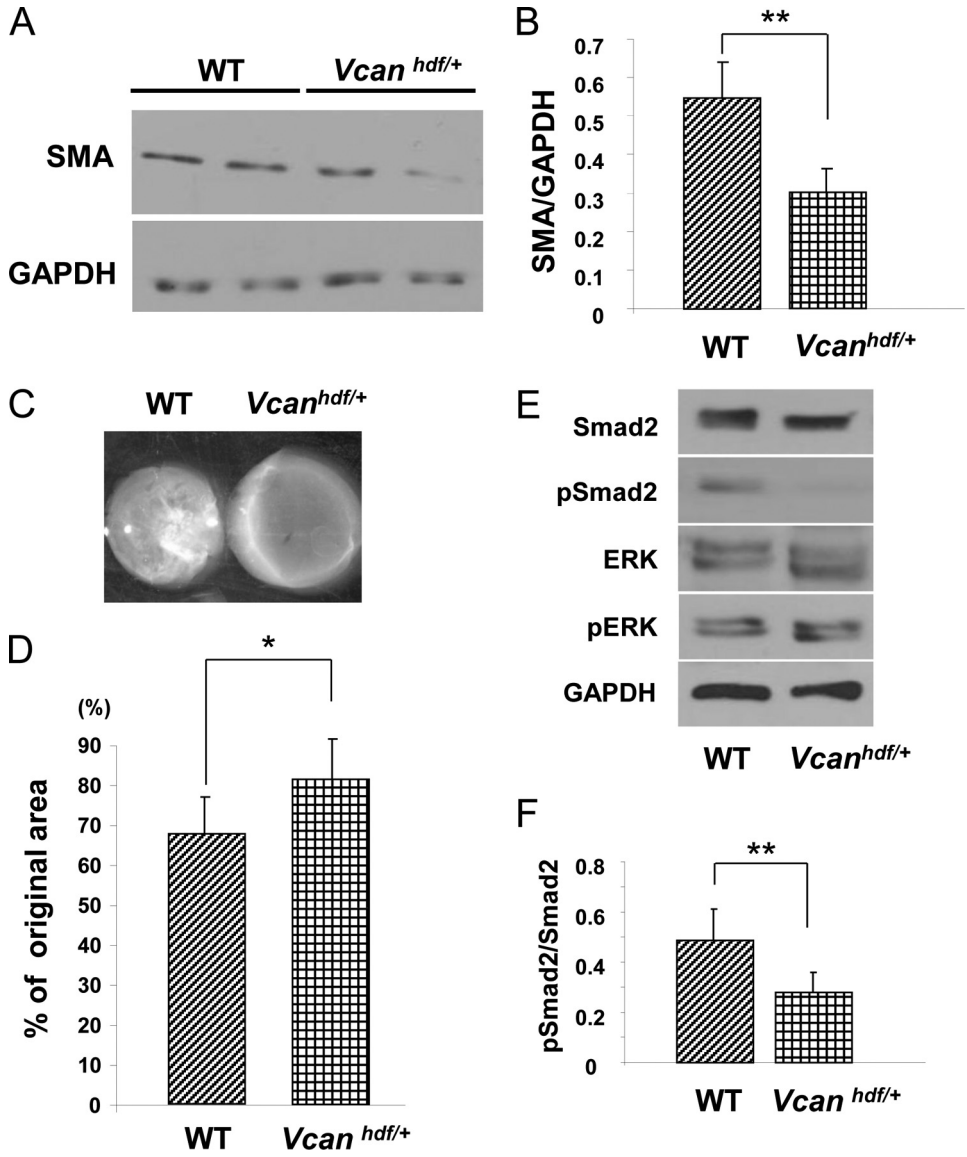


FIGURE 5. ***Vcan*$^{hdf/+}$ dermal fibroblasts have reduced SMA, reduced contractility, and decreased pSMAD2 activation *in vitro*.** *A*, a Western blot shows reduced SMA levels in *Vcan*$^{hdf/+}$ dermal fibroblasts (representative of three biological replicates and five technical replicates; see also supplemental Fig. 3). *B*, quantification of SMA levels shows a statistically significant reduction of SMA in *Vcan*$^{hdf/+}$ dermal fibroblasts (, **$p < 0.05$). *C*, a representative collagen gel contraction assay shows reduced ability of *Vcan*$^{hdf/+}$ dermal fibroblasts to contract a collagen gel compared with WT fibroblasts. *D*, quantification of collagen gel contraction shows a statistically significant reduction in contractility by *Vcan*$^{hdf/+}$ dermal fibroblasts compared with WT fibroblasts (*, $p < 0.01$, $n = 3$ biological replicates with triplicate wells per experiment). *E*, Western blot analysis shows decreased pSmad2 levels in *Vcan*$^{hdf/+}$ dermal fibroblasts but no effect on pERK levels. *F*, quantification of the ratio of pSmad2 to total Smad2 (obtained by densitometry of Western blots) shows a statistically significant decrease of Smad2 phosphorylation in *Vcan*$^{hdf/+}$ dermal fibroblasts (*, $p < 0.01$, $n = 3$ biological replicates).

sient transfection with an expression plasmid encoding full-length versican V1. Overexpression was confirmed by Western blot analysis, which demonstrated higher levels of the 350-kDa versican core protein after deglycosylation with chondroitinase ABC and 70-kDa ADAMTS-cleaved versican product (Fig. 7*A*). *Vcan* overexpressing cells had higher levels of SMA (Fig. 7, *B* and *C*) as well as enhanced contractility compared with fibroblasts transfected with the vector only (Fig. 7, *D* and *E*). Consistent with these observations of reduced versican processing and increased intact versican in *Adamts5*$^{-/-}$ cells, particle exclusion assays showed enhanced PCM around *Vcan* overexpressing cells (supplemental Fig. 7*A*, *arrows*) associated with increased pSMAD2 (Fig. 7*A*). Morphometric analysis indicated that *Vcan* overexpressing cells had an expanded surface area and a significantly reduced minor/major aspect ratio, which is a measure of the degree of spreading (supplemental Fig. 7, *B* and *C*). Thus, *Vcan* overexpression recapitulated the phenotype present in *Adamts5*$^{-/-}$ cells.

## DISCUSSION

Because of its pivotal location at the interface between the cell and its environment, the PCM occupies a potentially critical niche in cellular regulation, and it is possible that changes in either its volume or composition could influence cell behavior. Therefore, regulatory mechanisms that govern PCM assembly, content, and disassembly are potentially of broad significance to most cell types. CD44 and HA provide the foundation for formation of PCM in most cell types, and as shown here and

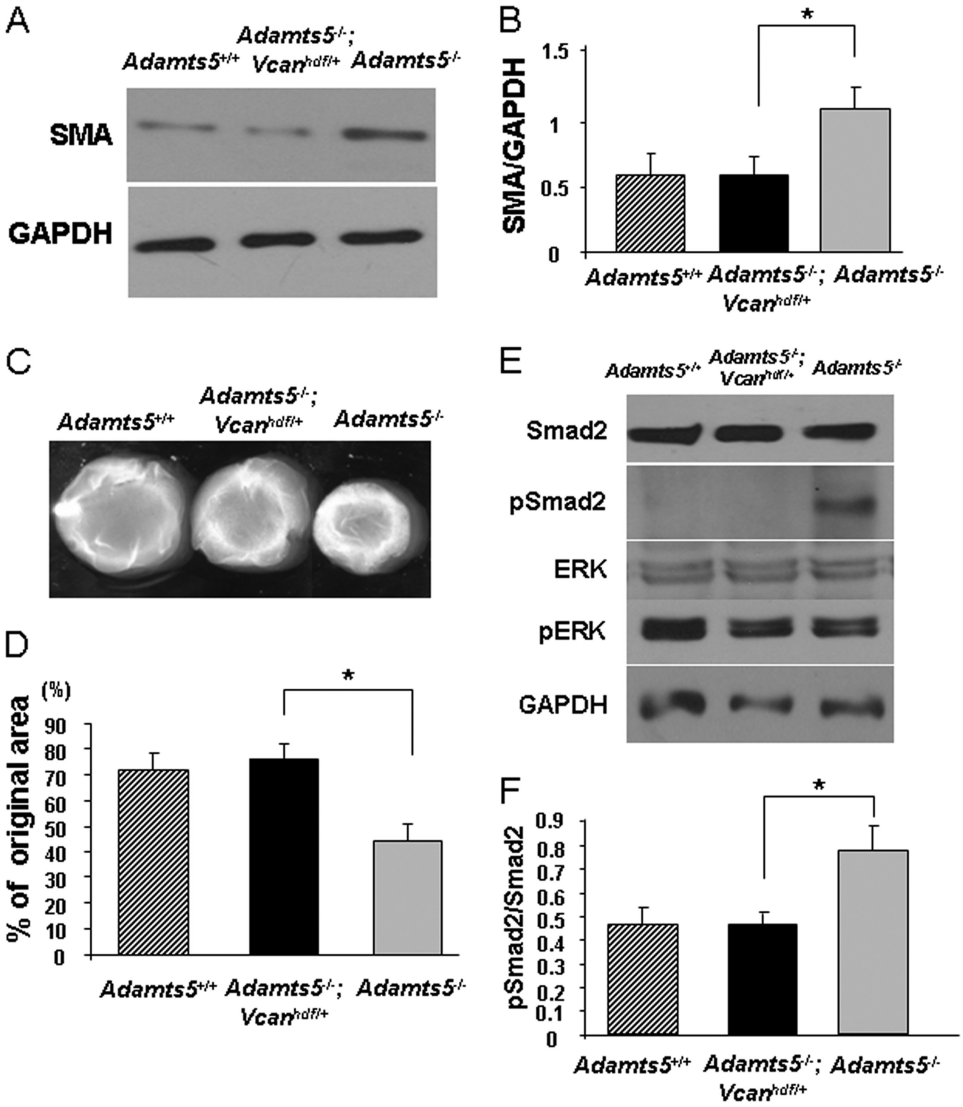


FIGURE 6. ***Vcan* haploinsufficiency abrogates the myofibroblast phenotype of *Adamts5*$^{-/-}$ dermal fibroblasts.** *A*, a representative Western blot analysis for SMA shows that the enhanced levels seen in *Adamts5*$^{-/-}$ cells are restored to those of WT fibroblasts by *Vcan* haploinsufficiency. *B*, quantification of SMA by densitometry of Western blots shows restoration of the increased levels in *Adamts5*$^{-/-}$ cells to WT levels by *Vcan* haploinsufficiency ($n = 3$). *C*, representative collagen gel contraction assay shows that the increased contractility of *Adamts5*$^{-/-}$ cells is reduced by *Vcan* haploinsufficiency, to be similar to that of WT cells. *D*, quantification of collagen gel contraction illustrates the restoration of contractility to the level of WT fibroblasts in *Adamts5*$^{-/-}$;*Vcan*$^{hdf/+}$ cells. *E*, Western blot analysis shows that increased pSmad2 in *Adamts5*$^{-/-}$ cells is reduced by *Vcan* haploinsufficiency. *F*, quantification of the ratio of pSmad2 to total Smad2 (obtained by densitometry of Western blots) shows a statistically significant decrease in Smad2 phosphorylation in *Adamts5*$^{-/-}$;*Vcan*$^{hdf/+}$ dermal fibroblasts compared with *Adamts5*$^{-/-}$ fibroblasts. *Error bars* indicate S.D.

elsewhere (10), the attached CSPG is also crucial. Chondrocytes, which synthesize the most voluminous PCM, express aggrecan (6), which is more heavily glycosylated than versican and may account at least in part for the greater PCM volume of chondrocytes relative to other cell types. Under unstimulated conditions, fibroblasts and vascular smooth muscle cells do not assemble a conspicuous PCM (13, 35), consistent with the observation in WT fibroblasts made here. Analysis of vascular smooth muscle cells demonstrated that development of a versican-HA PCM was required for proliferation and migration and could be induced by treatment with platelet-derived growth factor, whereas in fibroblasts, PCM was shown to be inducible by TGF$\beta$ (13, 36). The dynamic nature of PCM remodeling noted in vascular smooth muscle cells (13, 36) implied the existence of mechanisms for turnover of the CD44-HA-versican complex. However, neither the role of versican nor the mechanisms of its turnover in fibroblast PCM was previously investigated. In the present study we investigated the role of versican *per se* in PCM and in regulation of cell behavior. Closely integrated with this analysis, we determined the consequence of modification of PCM by ADAMTS5, a critical versican-degrading protease that is expressed by dermal fibroblasts.

The present work shows that, as in human skin (31), both the V0 and V1 isoforms of versican are present in murine skin. That these isoforms are turned over by ADAMTS proteases was shown by identification of anti-DPEAAE-reactive fragments detected in the DEAE-Sephacel pools. However, the V1 isoform was more abundant in dermal fibroblast cultures, as the cleaved and intact forms of this, but not of the V0 isoform, were detected. Analysis of dermal fibroblasts provided a strong asso-

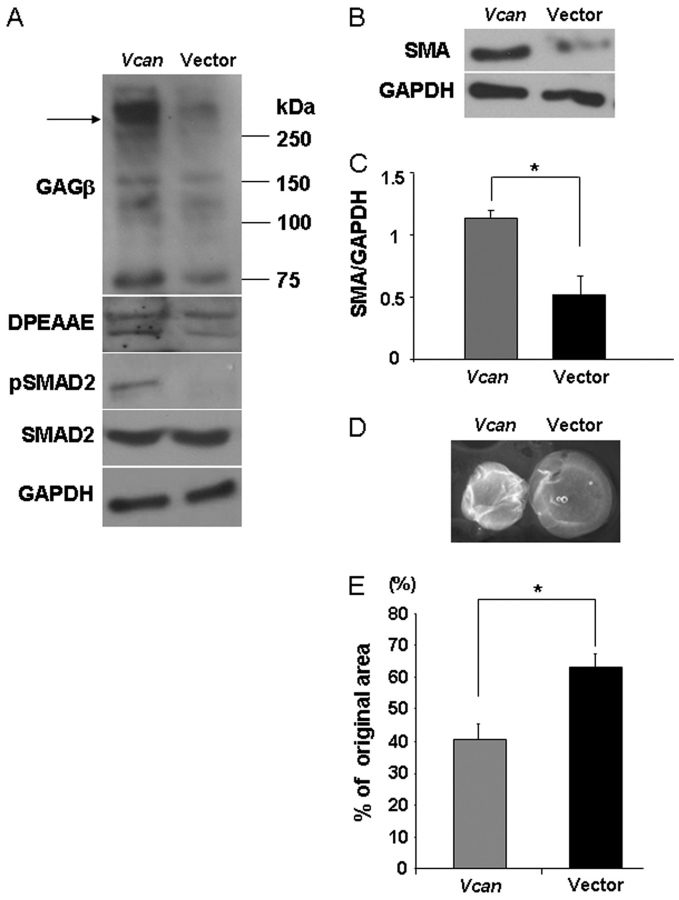


FIGURE 7. **Versican overexpression induces transition of normal human dermal fibroblasts to a myofibroblast phenotype.** *A*, Western blotting of cell monolayers with an antibody to versican (anti-GAG$\beta$) shows that increased versican V1 isoform expression (*arrow*) was achieved by transient transfection. Versican migrates as an ~350-kDa species when deglycosylated with chondroitinase ABC (*arrow*, *upper panel*) Coincident with this, there were increased levels of DPEAAE and pSMAD2 immunoreactivity (representative of $n = 2$). *B*, *Vcan*-overexpressing cells had increased levels of SMA (*center panel*) (representative of $n = 3$). *C*, quantification of SMA by densitometry of Western blots shows expression of significantly higher levels in normal human dermal fibroblasts by *Vcan* overexpression (*, $p < 0.01$, $n = 3$). *D*, collagen gel contraction assay showed that *Vcan*-overexpressing cells can contract a collagen gel to a greater extent. *E*, quantification of collagen gel contraction assay shows that V1 versican-overexpressing cells are contractile to a greater extent than control vector-transfected cells (*, $p < 0.01$, $n = 3$ independent transfections with three gels per experiment). *Error bars* indicate S.D.

ciation between reduced versican V1 processing in *Adamts5*$^{-/-}$ cells, increased PCM, altered cell morphology, and myofibroblast transition. Because versican is a known substrate of ADAMTS5, we considered whether accumulation of uncleaved versican could directly provide a mechanism for increased PCM. Indeed, the amelioration of myofibroblast characteristics by reducing the versican level in *Adamts5*$^{-/-}$ cells strengthens the possibility that the effects of ADAMTS5 deficiency are mediated at least in part by reduced versican processing. Additional support favoring a pivotal role for versican in PCM came from the finding that *Vcan*-haploinsufficient cells had reduced contractility in collagen gels and that overexpression of versican led to increased contractility. These experiments unequivocally showed that modulating versican content could have profound effects on cell behavior. In this work changing the versican content or altering ADAMTS5 levels also affected the canonical TGF$\beta$ signaling pathway, as indicated by altered Smad phosphorylation. The molecular basis for this is presently unclear, although previous work on versican suggests potential as well as indirect mechanisms. Specifically, it was recently shown that versican-deficient limb bud mesenchyme in the interzone demarcating the joints between developing bones bound TGF$\beta$ inefficiently and that versican core protein bound to TGF$\beta$ (37). In addition, versican binds to fibrillin-1, which interacts with the large latent complex of TGF$\beta$ formed by binding of TGF$\beta$ to latent TGF$\beta$-binding proteins (16). Thus, accumulation of versican in PCM could conceivably influence sequestration and/or activation of TGF$\beta$. Determination of the relationship between TGF$\beta$ and versican requires further detailed analysis.

TGF$\beta$ is a potent factor for conversion of a fibroblast to a myofibroblast (38). The myofibroblast is a phenotypically altered fibroblast that is characterized by increased expression of SMA and enhanced contractility (38). Myofibroblasts are formed either by transition from tissue fibroblasts or by epithelium to mesenchyme transformation (39). Fibroblast to myofibroblast transition occurs physiologically during skin wound healing, but the myofibroblast phenotype does not normally persist after healing. In contrast, myofibroblast conversion may persist in pathologic situations such as hypertrophic scarring, contractures after burns, and systemic and cutaneous scleroderma as well as in fibrosis of internal organs such as the lung, kidney, and liver (39). Organ-specific as well as systemic scleroderma is associated with high morbidity and mortality and presents a severe treatment challenge. Hence, factors that regulate the myofibroblast phenotype are of high medical significance. The present work identified ADAMTS5 and versican as novel, critical factors involved in the dermal fibroblast-myofibroblast transition and extends and complements the previous emphasis on HA. In establishing the key role of HA in the context of myofibroblast formation (35, 40–42) the role of the attached proteoglycan, which was likely to have been versican, was not addressed. It was shown that TGF$\beta$-induced conversion of dermal fibroblasts to myofibroblasts was associated with accumulation of HA in PCM and that inhibition of HA synthesis could modulate the response of the dermal fibroblast to TGF$\beta$ (35). However, the possible role of versican, the HA binding CSPG in most non-neural cell types other than chondrocytes was not previously investigated.

Interestingly, despite the consistent evidence for myofibroblast transition in cultured dermal *Adamts5*$^{-/-}$ fibroblasts, analysis of intact skin under base line conditions did not disclose an increase of SMA staining. Because multiple versican-degrading ADAMTS proteases are expressed in skin, it is possible that there is compensation by another ADAMTS in intact skin. The effect of ADAMTS5 deficiency might, therefore, remain latent unless coupled with deletion of other ADAMTS proteases or uncovered by skin wound healing or inflammation. In this context a recent study using a different strain of *Adamts5*$^{-/-}$ mice identified delayed wound closure in the absence of *Adamts5* and also suggested an accumulation of PCM, comprising aggrecan, not versican, in the fibroblasts occupying the healed dermis (43). In contrast to our data, neonatal dermal fibroblasts from the mutant mice had suppressed

TGF$\beta$ signaling (43). This publication did not analyze the effect of altering versican levels but showed that many of the observed effects could be ameliorated by deletion of CD44, hence, also potentially implicating PCM accumulation via a CD44-HA backbone (43). The differences between the published study and ours are intriguing and will need to be addressed by specific analysis of wound healing in the strain of mice we used.

Recent work using genetically targeted mice implicated several ADAMTS proteases in versican clearance in several biological processes. These included ovulation (ADAMTS1) (44), interdigital web regression (ADAMTS5, ADAMTS9, ADAMTS20) (25), endocardial cushion remodeling during valve development (ADAMTS5, ADAMTS9) (45, 46), palatogenesis (ADAMTS9, ADAMTS20) (47), melanoblast colonization of skin (ADAMTS20) (21), and endocardial jelly remodeling during myocardial compaction (ADAMTS1, ADAMTS9) (45, 48). These phenomena represent dramatic examples of tissue-sculpting involving the clearance of transitional, immature extracellular matrix rich in HA, and versican. In *Adamts5*$^{-/-}$ mice, we recently reported failure of remodeling of endocardial cushions during cardiac development, with persistence of versican; this defect was substantially rescued by the introduction of *Vcan* haploinsufficiency (46), a similar outcome as reported here.

Although a specialized extracellular matrix eventually replaces immature embryonic extracellular matrix, it is noteworthy that an HA- and versican-rich provisional matrix persists in and as the PCM, within which ADAMTS proteases could continue to have a role even in postnatal tissues, as demonstrated here. Previous work demonstrated that one or more bioactive versican fragments generated by ADAMTS proteases influenced specific developmental processes, such as interdigital sculpting and palate closure (25, 47). However, a putative versican bioactive fragment does not appear to have a role in versican modulation of the dermal fibroblast-myofibroblast for two reasons; first, versican haploinsufficiency substantially restored normal behavior in *Adamts5*$^{-/-}$ cells, and the addition of the N-terminal G1-DPEAAE$^{441}$ fragment generated by ADAMTS proteolysis did not restore the wild type fibroblast phenotype in *Adamts5*$^{-/-}$ cells.

Through a combination of cell biology and genetics, the present work has demonstrated the significance of versican, its proteolytic turnover in the fibroblast PCM, and its functional significance in dermal fibroblasts, which are potentially highly relevant to dermal fibrosis and skin wound healing. Because versican is a component of the PCM of many cell types, (49), the present work has broad implications. Versican-degrading ADAMTS proteases, including ADAMTS5 (28), are expressed in vascular smooth muscle cells, neurons, and cancer cells, and thus the levels of versican and/or ADAMTS activity may also modify the behavior of these cells. Indeed, the present work has therapeutic potential in that versican and ADAMTS levels could be potentially manipulated in these cells to achieve desired outcomes.

*Acknowledgments—We thank Dr. Hannah Bader for advice on the collagen gel contraction assay, Dr. Dieter Zimmermann for providing the versican expression plasmid, and Dr. Vincent C. Hascall for helpful comments on the manuscript.*

## REFERENCES


1. Clarris, B. J., and Fraser, J. R. (1967) *Nature* **214,** 1159
2. Clarris, B. J., and Fraser, J. R. (1968) *Exp. Cell Res.* **49,** 181–193
3. Bennett, H. S. (1963) *J. Histochem. Cytochem.* **11,** 14–23
4. Camaioni, A., Salustri, A., Yanagishita, M., and Hascall, V. C. (1996) *Arch. Biochem. Biophys.* **325,** 190–198
5. Evanko, S. P., Tammi, M. I., Tammi, R. H., and Wight, T. N. (2007) *Adv. Drug Deliv. Rev.* **59,** 1351–1365
6. Knudson, C. B. (1993) *J. Cell Biol.* **120,** 825–834
7. Maleski, M., and Hockfield, S. (1997) *Glia* **20,** 193–202
8. Van Teeffelen, J. W., Brands, J., Stroes, E. S., and Vink, H. (2007) *Trends Cardiovasc. Med.* **17,** 101–105
9. Thompson, W. R., Modla, S., Grindel, B. J., Czymmek, K. J., Kirn-Safran, C. B., Wang, L., Duncan, R. L., and Farach-Carson, M. C. (2011) *J. Bone Miner. Res.* **26,** 618–629
10. Knudson, W., and Knudson, C. B. (1991) *J. Cell Sci.* **99,** 227–235
11. Kultti, A., Rilla, K., Tiihonen, R., Spicer, A. P., Tammi, R. H., and Tammi, M. I. (2006) *J. Biol. Chem.* **281,** 15821–15828
12. Poole, C. A., Flint, M. H., and Beaumont, B. W. (1987) *J. Orthop. Res.* **5,** 509–522
13. Evanko, S. P., Angello, J. C., and Wight, T. N. (1999) *Arterioscler. Thromb. Vasc. Biol.* **19,** 1004–1013
14. Aspberg, A., Adam, S., Kostka, G., Timpl, R., and Heinegård, D. (1999) *J. Biol. Chem.* **274,** 20444–20449
15. Aspberg, A., Binkert, C., and Ruoslahti, E. (1995) *Proc. Natl. Acad. Sci. U.S.A.* **92,** 10590–10594
16. Isogai, Z., Aspberg, A., Keene, D. R., Ono, R. N., Reinhardt, D. P., and Sakai, L. Y. (2002) *J. Biol. Chem.* **277,** 4565–4572
17. Kuznetsova, S. A., Issa, P., Perruccio, E. M., Zeng, B., Sipes, J. M., Ward, Y., Seyfried, N. T., Fielder, H. L., Day, A. J., Wight, T. N., and Roberts, D. D. (2006) *J. Cell Sci.* **119,** 4499–4509
18. Olin, A. I., Mörgelin, M., Sasaki, T., Timpl, R., Heinegård, D., and Aspberg, A. (2001) *J. Biol. Chem.* **276,** 1253–1261
19. Longpré, J. M., McCulloch, D. R., Koo, B. H., Alexander, J. P., Apte, S. S., and Leduc, R. (2009) *Int. J. Biochem. Cell Biol.* **41,** 1116–1126
20. Sandy, J. D., Westling, J., Kenagy, R. D., Iruela-Arispe, M. L., Verscharen, C., Rodriguez-Mazaneque, J. C., Zimmermann, D. R., Lemire, J. M., Fischer, J. W., Wight, T. N., and Clowes, A. W. (2001) *J. Biol. Chem.* **276,** 13372–13378
21. Silver, D. L., Hou, L., Somerville, R., Young, M. E., Apte, S. S., and Pavan, W. J. (2008) *PLoS Genet.* **4,** 1–15
22. Somerville, R. P., Longpre, J. M., Jungers, K. A., Engle, J. M., Ross, M., Evanko, S., Wight, T. N., Leduc, R., and Apte, S. S. (2003) *J. Biol. Chem.* **278,** 9503–9513
23. Kuno, K., Terashima, Y., and Matsushima, K. (1999) *J. Biol. Chem.* **274,** 18821–18826
24. Gao, G., Plaas, A., Thompson, V. P., Jin, S., Zuo, F., and Sandy, J. D. (2004) *J. Biol. Chem.* **279,** 10042–10051
25. McCulloch, D. R., Nelson, C. M., Dixon, L. J., Silver, D. L., Wylie, J. D., Lindner, V., Sasaki, T., Cooley, M. A., Argraves, W. S., and Apte, S. S. (2009) *Dev. Cell* **17,** 687–698
26. Mjaatvedt, C. H., Yamamura, H., Capehart, A. A., Turner, D., and Markwald, R. R. (1998) *Dev. Biol.* **202,** 56–66
27. Cheng, G., Swaidani, S., Sharma, M., Lauer, M. E., Hascall, V. C., and Aronica, M. A. (2011) *Matrix Biol.* **30,** 126–134
28. McCulloch, D. R., Le Goff, C., Bhatt, S., Dixon, L. J., Sandy, J. D., and Apte, S. S. (2009) *Gene Expr. Patterns* **9,** 314–323
29. Koo, B. H., Coe, D. M., Dixon, L. J., Somerville, R. P., Nelson, C. M., Wang, L. W., Young, M. E., Lindner, D. J., and Apte, S. S. (2010) *Am. J. Pathol.* **176,** 1494–1504
30. Carrino, D. A., Sorrell, J. M., and Caplan, A. I. (2000) *Arch. Biochem. Biophys.* **373,** 91–101
31. Carrino, D. A., Calabro, A., Darr, A. B., Dours-Zimmermann, M. T., Sandy, J. D., Zimmermann, D. R., Sorrell, J. M., Hascall, V. C., and Caplan, A. I. (2011) *Glycobiology* **21,** 257–268
32. Carrino, D. A., Arias, J. L., and Caplan, A. I. (1991) *Biochem. Int.* **24,** 485–495

33. Oike, Y., Kimata, K., Shinomura, T., Nakazawa, K., and Suzuki, S. (1980) *Biochem. J.* **191,** 193–207
34. Lauer, M. E., Mukhopadhyay, D., Fulop, C., de la Motte, C. A., Majors, A. K., and Hascall, V. C. (2009) *J. Biol. Chem.* **284,** 5299–5312
35. Meran, S., Thomas, D., Stephens, P., Martin, J., Bowen, T., Phillips, A., and Steadman, R. (2007) *J. Biol. Chem.* **282,** 25687–25697
36. Evanko, S. P., Johnson, P. Y., Braun, K. R., Underhill, C. B., Dudhia, J., and Wight, T. N. (2001) *Arch. Biochem. Biophys.* **394,** 29–38
37. Choocheep, K., Hatano, S., Takagi, H., Watanabe, H., Kimata, K., Kongtawelert, P., and Watanabe, H. (2010) *J. Biol. Chem.* **285,** 21114–21125
38. Wynn, T. A. (2008) *J. Pathol.* **214,** 199–210
39. Abraham, D. J., and Varga, J. (2005) *Trends Immunol.* **26,** 587–595
40. Meran, S., Thomas, D. W., Stephens, P., Enoch, S., Martin, J., Steadman, R., and Phillips, A. O. (2008) *J. Biol. Chem.* **283,** 6530–6545
41. Webber, J., Jenkins, R. H., Meran, S., Phillips, A., and Steadman, R. (2009) *Am. J. Pathol.* **175,** 148–160
42. Webber, J., Meran, S., Steadman, R., and Phillips, A. (2009) *J. Biol. Chem.* **284,** 9083–9092
43. Velasco, J., Li, J., Dipietro, L., Stepp, M. A., Sandy, J. D., and Plaas, A. (2011) *J. Biol. Chem.* **286,** 26016–26027
44. Brown, H. M., Dunning, K. R., Robker, R. L., Boerboom, D., Pritchard, M., Lane, M., and Russell, D. L. (2010) *Biol. Reprod.* **83,** 549–557
45. Kern, C. B., Wessels, A., McGarity, J., Dixon, L. J., Alston, E., Argraves, W. S., Geeting, D., Nelson, C. M., Menick, D. R., and Apte, S. S. (2010) *Matrix Biol.* **29,** 304–316
46. Dupuis, L. E., McCulloch, D. R., McGarity, J. D., Bahan, A., Weber, D., Diminich, A. M., Wessels, A., Nelson, C. M., Apte, S. S., and Kern, C. B. (2011) *Dev. Biol.* **357,** 152–164
47. Enomoto, H., Nelson, C. M., Somerville, R. P., Mielke, K., Dixon, L. J., Powell, K., and Apte, S. S. (2010) *Development* **137,** 4029–4038
48. Stankunas, K., Hang, C. T., Tsun, Z. Y., Chen, H., Lee, N. V., Wu, J. I., Shang, C., Bayle, J. H., Shou, W., Iruela-Arispe, M. L., and Chang, C. P. (2008) *Dev. Cell* **14,** 298–311
49. Ricciardelli, C., Russell, D. L., Ween, M. P., Mayne, K., Suwiwat, S., Byers, S., Marshall, V. R., Tilley, W. D., and Horsfall, D. J. (2007) *J. Biol. Chem.* **282,** 10814–10825